A CFD study of the behavior of a crew transfer vessel in head seas using OpenFOAM

Yujia Wei[a] and Tahsin Tezdogan[a,*]

[a] Department of Naval Architecture, Ocean and Marine Engineering, Henry Dyer Building, University of Strathclyde, 100 Montrose Street, Glasgow, G4 0LZ, UK

Abstract

Crew transfer vessels (CTV) were a fast means of transportation, providing inspection and maintenance services by transferring technicians from shore to offshore structures. These vessels had been designed to be efficient and effective at high speeds, though this means the ship motions were highly sensitive to the sea conditions. Accordingly, it was critical to be able to estimate a ship's response among different wave conditions in the time domain. In this study, a Computational Fluid Dynamics (CFD) method was used for the analysis of Fluid-Structure interactions with a crew transfer vessel as a case study. The CFD codes were formulated to solve the unsteady Reynolds-Averaged Navier–Stokes equations using the finite-volume method with OpenFOAM, an open-source CFD software program. OpenFOAM offered high accuracy of ship motion predictions and high resolution of infield flow phenomena, taking into consideration both viscous and rotational effects in the flow and free surface waves. A comprehensive uncertainty analysis was presented, including verification and validation studies. The cases performed demonstrate that the results were found to be in good agreement with the available experimental results and showed the importance of a seakeeping analysis for such vessels.

Keywords: Computational Fluid Dynamics, Crew Transfer Vessel, Motion, Turbulence

1. Introduction

Crew transfer vessels, as applicable to the offshore wind industry, were mainly a type of catamaran with a size between 16 meters to 27 meters, providing maintenance services by transferring technicians from port to offshore wind platforms. The double-hull featured vessels had less hull volume, small displacement and low drag in the water, which benefited the high mobility and fuel economics. During the transfer phase, the seakeeping characteristics need more attention, as Phillips, et al., [1] stated that technicians may be more sensitive to get the motion sickness effects than seamen. There were several

* Corresponding author E-mail address: tahsin.tezdogan@strath.ac.uk (T. Tezdogan)

existing guidelines [9][10][11] which illustrated the operational limits of a crew transfer sailing at sea conditions with the consideration of the crew comforts, the corresponding criteria were listed:

1. The vertical acceleration a_{CG} at LCG was less than 0.15g [9][10], and horizontal acceleration was about 0.12g [1].
2. The maximum significant wave height was 1.5m, noting that the operational ability was also affected by the wave frequency, wave length and current [10].
3. The maximum pitch and roll RMS values were 4 degrees and 6 degrees, respectively [1].

Generally, the accurate prediction of ship motion was the primary importance to study on the transferability and accessibility of CTV operation at seas.

With particular regard to the seakeeping behavior of a ship, computational fluid dynamics (CFD) had gained high popularity for such predictions due to low cost comparing with the experimental fluid dynamics (EFD) procedures. There were many studies presented in this field. In the Gothenburg 2000 workshop [12], three ship models the KCS, the KVLCC and the DTMB 5415 were studied based on the verification and validation results. In the latter workshop at Gothenburg 2010 [13], the evaluation of local flow predictions and seakeeping predictions were further analyzed for the same ship geometry provided by the workshop of 2000. Tezdogan et al., 2015 [2] compared the CFD, the potential flow-based method, and the model experiment results with respect to full-scale KCS in low-speed sailing, and then analyzed the differences among ship motions, total resistance and added resistance. In addition, the double-hull ship's motions were investigated by many researchers. Sahoo et al., 2007 [5] presented a regression analysis based on the CFD method to compute the wave-making resistance of a catamaran and compared with the experimental results. Moraes et al., 2004 [14] studied the catamaran hull resistance in deep and shallow waters for different hull shapes and spacing based on the slender-body theory and a 3D CFD method software package. Castiglione et al., 2011 [15] presented the seakeeping behavior of a catamaran in head wave using an unsteady RANS code with the level set approach to capture the free surface. In their study, ship motions were solved with the rigid body equations. The in-house RANs solver "naoe-FOAM_SJTU" developed by Shanghai JiaoTong University was used on modelling the catamaran resistance in calm water. The vorticity around the ship geometry was visualized at the near-wall region [16].

In this paper, the open-source CFD libraries "OpenFOAM" were studied on the prediction of the catamaran motions in wave heights of up to 1.7m. A brief introduction of the model and solver settings

were presented in Section 2. Then a verification and validation (V&V) was studied to investigate the solver capability in Section 3.

2.Solution process

2.1 Solver description

"WaveDyFoam" was used in this study as a fluid solver. It was an interFoam-extend, merging wave generating library "waves2Foam" [3] and moving mesh technique, then coupled with the standard volume of fluid (VOF) scheme. Ship was assumed to be rigid body, and the motion is calculated basing on the default structure solver "sixDoFRigidBodyMotion" in OpenFOAM.

2.2 Ship specifications

The research vessel used in this study was a double-hull catamaran that had a length of 18m, and a light draft of 1.38m, which were common types used for providing services among wind farms. The ship model used in this analysis received from the hydrodynamic lab of the University of Strathclyde with a scale ratio of 1:10 [17]. The vessel parameters were verified with several experimental tests before, including the weighting, inclining and swing test [17]. The vessel's main particulars in model scale were shown in Table 1 and its hull form was demonstrated in table 1.

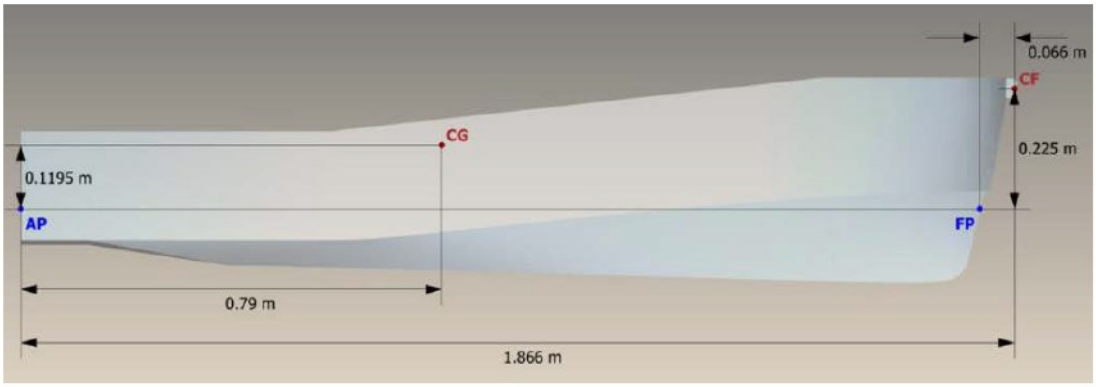

Figure 1: Body plane of the catamaran model

Table 1: The principal particulars of a catamaran ship

Principal particulars	Symbol	Scale
Scale factor	λ(-)	10
Length	$L(m)$	1.85

Breath	$B(m)$	0.69
Design draft	$T(m)$	0.138
Displacement volume	$\nabla(m^3)$	0.044293
Vertical center of gravity (from keel)	$KG(m)$	0.253
Moment of inertia	$k_{yy}(\mathrm{kg}m^2)$	9.157
Reynolds number	R_e(-)	4.26×10^7

2.3 Boundary conditions

The wave domain used in this case represented a deep water condition, therefore, the lateral sides and bottom boundaries were set as symmetry plane. The detailed boundary conditions setting was listed in Table 2. Basic boundary condition, FV for Fixed value (Dirichlet), and ZG for zero gradient (Neumann) were mainly set for the inlet and outlet. PIOV was pressure Inlet Outlet Velocity that assigned a zero gradient condition for flow out of the domain, whilst assigned a velocity based on the flux normal for flow into the domain. FFP was fixed Flux Pressure, used for pressure in situations where the zero gradient was generally used. IO was an inlet Outlet that assigned a zero gradient condition for outflow and a fixed value inflow. The corresponding turbulence wall functions were applied at the ship hull and the calculated implied a type of boundary condition which calculated field values based on other fields.

Table 2: Boundary conditions used in the simulation

	Inlet	Outlet	Atmosphere	catamaran
U	WV	ZG	PIOV	MWV
P_rgh	FFP	ZG	TP	FFP
a.water	WA	VHFR	IO	ZG
PointDisplacement	FV	FV	FV	Calculated
k	FV	ZG	IO	kqRWF
nut	FV	ZG	ZG	nutkWF
omega	FV	ZG	IO	omegaWF

2.4 Turbulent modelling

Turbulence was modelled with the Reynolds-averaged stress (RAS) SST $k-\omega$ model. The inlet turbulence parameters were calculated and assigned at the initial condition with the following equations which were used by Labanti et al., 2003 [12] and Islam et al., 2019 [19].

$$I = 0.16 \cdot Re^{-\frac{1}{8}} \quad (1)$$

$$k = \frac{3}{2}(u \cdot I)^2 \quad (2)$$

$$\delta = \frac{L}{\sqrt{Re}} \quad (3)$$

$$\mathrm{l} = 0.4 \cdot \delta \quad (4)$$

$$C_\mu = 0.09 \quad (5)$$

$$\omega = \frac{\sqrt{k}}{C_\mu^{1/4} \cdot l} \quad (6)$$

$$V_T = \sqrt{\frac{3}{2}} \cdot u \cdot I \cdot l \quad (7)$$

Where I was the turbulence intensity; k was the turbulent kinetic energy; δ was the height of the first adjacent layer; l was the turbulence length scale, ω was the turbulence specific dissipation rate, V_T was the turbulent kinetic eddy viscosity. $C_\mu = 0.09$ was a model coefficient of the $k-\epsilon$ and $k-\omega$ turbulence models.

2.5 Meshing

The hull form was generated by the "SnappyHexMesh" utility using a cell splitting and body fitting technique, which created unstructured hexahedral meshes around the hull surface from the specified STL file. The utility required a preliminary uniform background grid, and literately refined the mesh at the free surface and near-ship zones [2], the whole mesh layout was shown in Figure 2. The sub-layer meshes were generated outward normal to the ship surface, and the first adjacent wall was placed in the log-law region, in which the corresponding turbulence wall functions were required. The model stability and accuracy were highly dependent on the mesh quality, according to the ITTC requirements [8], the mesh skewness and non-orthogonality were the key factors, which restricted under 4 and 65 degrees in this case respectively.

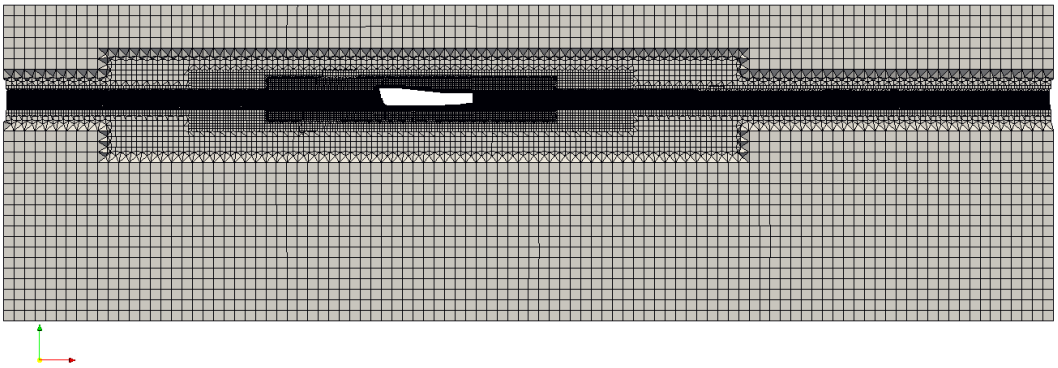

Figure 2: A cross-section of the computation mesh showing the refinement zone at near wall region and free surface.

2.6 Numerical methods

The time derivative term was discretized using the first order backward Euler scheme, which had been widely used in the industry. The second order linear upwind differencing scheme was set for convection terms. The artificial compression term was introduced to the phase fraction convection equation to exert pressure on the interface to keep it from dispersing [4]. The pressure-momentum coupling equations were solved based on the PIMPLE algorithm, which contained five sub-cycling for each time step with extra two pressure-correction inner loops. The cell motion was calculated for the mesh deformation technique. An overall relaxation factor of 0.9 was set for all variables to stabilize the numerical model.

2.7 Wave property

Accurate simulation of wave propagation was of primary importance for solving wave-structure interaction problems. The wave generating and absorption both used the relaxation technique, to avoided the wave reflection from the walls. The inlet relaxation zone took 1.0 wavelength windward the bow, and the outlet relaxation zone took 1.5 wavelength downstream the stern, as shown in Figure 3.

A second order stokes wave was used with the wave height of 0.017m throughout all simulations. The wave elevation was monitored by the numerical probe placing 3m in the front of the ship bow. A preparation study of only wave propagation inside the domain was presented, and one wave peak amplitude with four different grid numbers at the free surface was shown in Figure 4. It can be seen that the grid number 12 and 16 at the free surface both presented an accurate wave generating capability. The

comprehensive mesh convergence study was presented in Section 3.

Figure 3. Numerical wave domain with relaxation zones layout

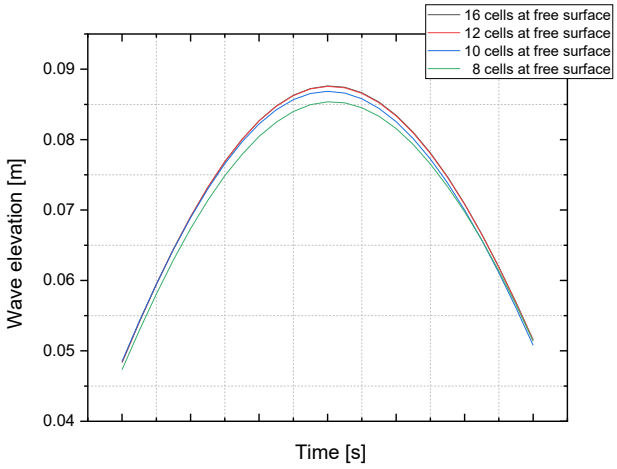

Figure 4: Wave elevation (peak) monitored at probe position (-4,0,0) with four different grids density at free surface

2.8 Computational resource

The simulations were run on Archie-West HPC (High-Performance Computation) cluster. The specification of HPC cluster was a 2560 cores (64 Lenovo SD530 nodes) with 192GB of RAM per node (4.8GB per core) using Intel Xeon Gold 6138 (Skylake) processors. All the cases were run parallel on a single node (40 cores), the average time step was set to be 0.002s. All the simulations were run up to 30s for attaining stable results and the required the physical time was about 120h -140h per case.

3. Verification and Validation

3.1 Verification study

The verification study was a substantiation procedure that a numerical model represented a conceptual model within specified limits of accuracy [6]. According to ITTC [20], the numerical errors had three categories into iterative errors, gird size error, time step errors [7][19]. The iterative error was mainly caused by the normalized residuals when solving PDE equations with the differential methods, as ITTC [8] regulated the convergence should be achieved with at least three orders of magnitude decrease of error. The iterative error may be ignored in this case due to the tolerance control setting were applied in the solver. Only the uncertainty of grid and time were presented based on the error estimation approach called Grid Convergence Method (GCI), which was first presented by Celik et al [21] based on the Richardson extrapolation (RE) method. It referred to overcome the limitation RE method that the predicted variables may not exhibit a smooth monotonic dependence on grid resolution. Three key factors were studied, the convergence ratio R_k, the order of accuracy p and the Grid Convergence Index (GCI). The convergence ratio implied the result difference between each two pair of cases, and the value was used to judge for the convergence conditions:

$$R_k = \epsilon_{21}/\epsilon_{32} \tag{8}$$

1. Monotonic convergence: $0 < R_k < 1$;
2. Oscillatory convergence: $R_k < 0$;
3. Divergence: $R_k > 1$

Where the ϵ_{21} and ϵ_{32} represented the solution differences of coarse case φ_1 and medium case φ_2, medium case φ_2 and fine case φ_3, the expression showed below.

$$\epsilon_{21} = \varphi_2 - \varphi_1 \tag{9}$$

$$\epsilon_{32} = \varphi_3 - \varphi_2 \tag{10}$$

The order of accuracy p and Grid Convergence Index (GCI) were predicted using the following equations:

$$p = \frac{1}{\ln(r_{21})}\left|\ln\left|\frac{\epsilon_{k32}}{\epsilon_{k21}}\right| + q(p)\right| \tag{11}$$

$$GCI_{fine}^{21} = \frac{1.25e_a^{21}}{r_{21}^p - 1} \tag{12}$$

For performing the uncertainty analysis, three different mesh resolutions and three time steps were used. For the mesh convergence test, the grid numbers were refined at the free surface, the number increased with a rough ratio of $\sqrt{2}$ among coarse, medium and fine cases, from 8 to 16. The total grid numbers were increased correspondingly from 5.41 million (10 cells) to 9.19 million (16 cells). Also, three time steps, 0.002s, 0.004s,0.008s were studied for the time convergence test, with an increasing ratio of 2. The GCI results were shown in Table 3, which were analyzed for the trim and sinkage prediction with the

ship has no forward speed and the wave period is 2s.

Table 3: The GCI uncertainty analysis performed for the catamaran model at wave frequency of 0.5 Hz

Mesh convergence study	Trim at COG [m]	Sinkage at COG [m]	Time convergence study	Trim at COG [m]	Sinkage at COG [m]
Coarse solution (f1)	0.0761	4.5808	Coarse solution (f1)	0.0771	4.6475
Medium solution (f2)	0.0757	4.591	Medium solution (f2)	0.0668	4.6220
Fine solution (f3)	0.0740	4.632	Fine solution (f3)	0.0613	4.2706
Number of coarse cells	4,492,152	4,492,152	Minimum time step	0.002	0.002
Number of medium cells	5,906,328	5,906,328	Medium time step	0.004	0.004
Number of fine cells	9,186,726	9,186,726	Maximum time step	0.008	0.008
Refinement ratio r21	0.76057	0.76057	Refinement ratio r21	2	2
Refinement ratio r32	0.64292	0.64292	Refinement ratio r32	2	2
Convergence ratio R	0.23529	0.24878	**Convergence ratio R**	1.8727	0.066859
Value of s	-1	-1	Value of s	-1	-1
Order of accuracy	1.4325	1.3259	**Order of accuracy**	0.90514	3.9027
Value of function	-1.0549	-1.0283	Value of function	0	0
Relative error	0.52562%	0.22267%	Relative error	13.3593%	0.54868
Extrapolated result	0.076933	4.5575	Extrapolated result	0.088902	4.6493
Extrapolated error	1.0831%	-0.51159%	Extrapolated error	13.2754%	0.039297%
GCI uncertainty	1.3687%	0.63623%	**GCI uncertainty**	19.1344%	0.049141%

As can be seen from the above analysis, the results showed three monotonous convergence cases and one divergence case for the time step. It may occur because the maximum time step was selected too large, which cannot resolve the fluid field properly, thus a divergence convergence was observed.

3.2 Validation study

The validation study presented here was the FFT evaluated results of the ship heave and pitch transfer functions with five wave frequencies. The medium-mesh grid density (12 grids at the free surface) and the smallest time steps (0.002s) were selected through all simulations. The numerical results (black) were

compared with the experimental result (red), as shown in Figure 5. The numerical results showed a good agreement with the experiments.

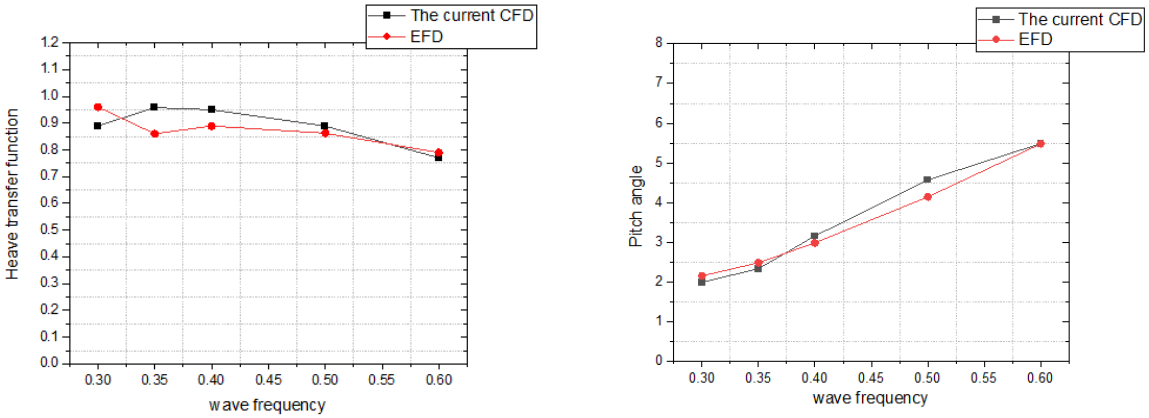

Figure 5: The heave and pitch results compared between numerical model and experiments.

For short wave or high frequency cases, especially $f > 0.6$Hz, the current CFD code had difficulties presenting accurate results because the smaller cells (high resolution mesh near hull surface) were deformed and failed quickly. Better dynamic mesh technique, e.g., Overset mesh, could be a good alternative for such cases.

To further illustrate the results, the stream velocity distribution at the free surface with four shot cuts was presented in Figure 6 for one wave period. The resulting wave pattern showed a high resolution at the boundary conditions, which proved the current mesh distribution was capable to capture the flow phenomenon at near-wall regions. It could be noted that the high flow velocity was monitored at the region between two demi hulls, which may cause by the water trapping phenomenon.

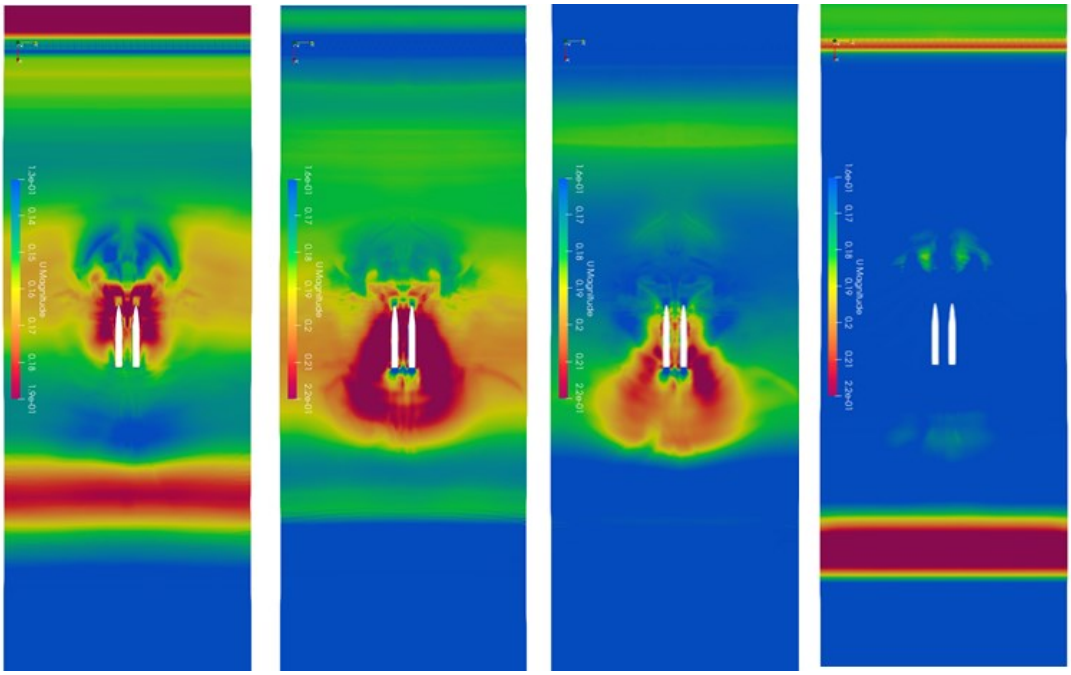

Figure 6: Velocity distribution on free surface and hull form for wave period at 2s.

4. Conclusion

This study showed the current CFD code capacity to predict a double-hull vessel motion in heading waves. Three different mesh resolution and three time steps were used to perform the numerical uncertainty analysis, then the results were compared with experimental data for validation.

The current dynamic mesh technique was not fully equipped to perform cases with well pronounced ship motions. Therefore, alternative mesh handling method was required for the cases with short wave period and large wave heights.

The prediction of the ship response in the critical wave height (1.7m) was presented in Figure 5, which showed that the ship motions were highly dependent on the wave frequency. The pitch angle was lower than 4 degrees when the wave frequency was less than 0.5 Hz. Therefore, this ship may be capable to perform operations in such circumstances.

5. Acknowledgement

The authors would like to acknowledge the numerical results were obtained using the ARCHIE-WeSt High Performance Computer (www.archie-west.ac.uk) based at the University of Strathclyde."

Reference:

1. Phillips, S., Shin, I. B., & Armstrong, C. (2015). Crew transfer vessel performance evaluation. *RINA, Royal Institution of Naval Architects - Design and Operation of Wind Farm Support Vessels 2015, Papers*, *January*, 29–33.
2. Tezdogan, T., Demirel, Y. K., Kellett, P., Khorasanchi, M., Incecik, A., & Turan, O. (2015). Full-scale unsteady RANS CFD simulations of ship behaviour and performance in head seas due to slow steaming. *Ocean Engineering*, *97*, 186–206. https://doi.org/10.1016/j.oceaneng.2015.01.011
3. Jacobsen, N. G., Fuhrman, D. R., & Fredsøe, J. (2012). A wave generation toolbox for the open-source CFD library: OpenFoam®. *International Journal for Numerical Methods in Fluids*, *70*(9), 1073–1088. https://doi.org/10.1002/fld.2726
4. Amini Afshar, Mostafs, (2010) Numerical Wave Generation In OpenFOAM®, Chalmers University of Technology.
5. Sahoo, P. K., Salas, M., & Schwetz, A. (2007). Practical evaluation of resistance of high-speed catamaran hull forms - Part I. *Ships and Offshore Structures*, *2*(4), 307–324. https://doi.org/10.1080/17445300701594237
6. Roy, C. J., & Oberkampf, W. L. (2016). Verification and validation in computational fluid dynamics. *Handbook of Fluid Dynamics: Second Edition*, *March*, 44.1-44.11. https://doi.org/10.1201/b19031-50
7. Stern, F., Wilson, R. V., Coleman, H. W., & Paterson, E. G. (2001). Comprehensive approach to verification and validation of CFD simulations—Part 1: Methodology and procedures. *Journal of Fluids Engineering, Transactions of the ASME*, *123*(4), 793–802. https://doi.org/10.1115/1.1412235
8. ITTC. (2014). Practical Guidelines for Ship CFD Applications ITTC –Recommended Procedures and Guidelines, section 7.5-03-02-03. *International Towing Tank Conference*.
9. DNV GL. (2015). *RULES FOR CLASSIFICATION High speed and light craft Part 1 General regulations Chapter 2 Class notations*. *December*, 1–23. http://rules.dnvgl.com/docs/pdf/DNVGL/RU-HSLC/2015-12/DNVGL-RU-HSLC-Pt1Ch2.pdf
10. Note, G. (2018). *Rules for the Classification of Crew Boat Guidance Note*. *33*(January).
11. G9 Offshore Wind Health and Safety Association., & Energy Institute (Great Britain). (n.d.). *G9 Safe by Design : workshop report : marine transfer/access systems.* 38.
12. Larsson, L., Stern, F., & Bertram, V. (2003). Benchmarking of computational fluid dynamics for ship flows: The Gothenburg 2000 workshop. Journal of Ship Research, 47(1), 63–81. https://doi.org/10.5957/jsr.2003.47.1.63
13. Wehausen, J. V., & Salvesen, N. (1977). Numerical ship hydrodynamics.
14. Moraes, H. B., Vasconcellos, J. M., & Latorre, R. G. (2004). Wave resistance for high-speed catamarans. Ocean Engineering, 31(17–18), 2253–2282. https://doi.org/10.1016/j.oceaneng.2004.03.012
15. Castiglione, T., Stern, F., Bova, S., & Kandasamy, M. (2011). Numerical investigation of the seakeeping behavior of a catamaran advancing in regular head waves. Ocean Engineering, 38(16), 1806–1822. https://doi.org/10.1016/j.oceaneng.2011.09.003
16. Zha, R. S., Ye, H. X., Shen, Z. R., & Wan, D. C. (2015). Numerical computations of resistance of high speed catamaran in calm water. Journal of Hydrodynamics, 26(6), 930–938. https://doi.org/10.1016/S1001-6058(14)60102-5
17. University of Strathclyde Department of Naval Architecture , Ocean and Marine Engineering Experimental Investigation Regarding the Landing Manoeuvre of a Crew Transfer Vessel

Zhaoxian Lin Supervisor : Prof . Osman Turan , Prof . Sandy Day March 2019 Ackno. (2019). March.

18. Stern, F., Wilson, R., & Shao, J. (2006). Quantitative V&V of CFD simulations and certification of CFD codes. International Journal for Numerical Methods in Fluids, 50(11), 1335–1355. https://doi.org/10.1002/fld.1090
19. ITTC – Recommended Procedures and Guidelines, 2008. Uncertainty Analysis in CFD Verification and Validation Methodology and Procedures. ITTC 7.5-03-01-01.
20. ITTC (2017). The seakeeping committee: final report and recommendations to 28th ITTC
21. Celik, I. B., Ghia, U., Roache, P. J., Freitas, C. J., Coleman, H., & Raad, P. E. (2008). Procedure for estimation and reporting of uncertainty due to discretization in CFD applications. *Journal of Fluids Engineering, Transactions of the ASME*, *130*(7), 0780011–0780014. https://doi.org/10.1115/1.2960953